Eur. Phys. J. Plus (2022) 137:324
https://doi.org/10.1140/epjp/s13360-022-02501-4

THE EUROPEAN PHYSICAL JOURNAL PLUS

Regular Article

Nonleptonic weak decays of B_c meson involving $B_{(s)1}$, $D_{(s)1}$ mesons

Rohit Dhir[1,a], **Neelesh Sharma**[1,2,b]

[1] Department of Physics and Nanotechnology, SRM Institute of Science and Technology, Kattankulathur 603203, India
[2] Paradigm of Science Cultivation and Ingenious, Kangra 176032, India

Received: 24 June 2021 / Accepted: 15 February 2022

Abstract We study the two-body weak decays of bottom-charm (B_c) and bottom-strange (B_s) mesons decay to a pseudoscalar meson (P) and an axial-vector meson (A) in CKM-favored and CKM-suppressed modes. We have obtained the form factors involving $B_c \to A_1^{1/2}$, $A_1^{3/2}$ and $B_s \to A_1^{1/2}$, $A_1^{3/2}$ transitions in the nonrelativistic quark model framework within the heavy quark symmetry constraints. The predictions of branching ratios for $B_c \to B_{(s)1}P$ and $B_c(B_s) \to D_{(s)1}P$ decays are presented. We find that the branching ratios of several decays are $\mathcal{O}(10^{-2}) \sim \mathcal{O}(10^{-5})$.

1 Introduction

Investigation of the two-body nonleptonic weak decays of bottom mesons can serve as an important tool to study the electroweak physics, hadronic structure, and physics beyond the standard model (SM). Another interesting aspect of such studies is to explore the heavy flavor dynamics (that involves nonperturbative quantum chromodynamics (QCD)) to construe electroweak and new physics from heavy quark decays [1–7]. Furthermore, the decays of heavy mesons provide a great opportunity to explore the exotic hadronic states beyond the naive quark model [8]. It is well known that the phenomenology involving heavy quark effective theory (HQET) along with the factorization hypothesis has been successfully employed to study the heavy meson decays [5–7]. The analysis of decays involving $B_q \to D_{(s)}^{**}P$ transitions, where $q \equiv \{s,\ c\}$ quarks and $D_{(s)}^{**} \equiv \{D_{(s)0}, D_{(s)1}, D_{(s)2}\}$ ($p-$wave) mesons, provides an opportunity to test HQET and heavy quark symmetry (HQS) in $m_Q \to \infty$ limit [9–13]. The B_c meson decays are of special interest as compared to the flavor-neutral heavy quarkonium ($b\bar{b}$, $c\bar{c}$) states, as it only decays *via* weak interactions, while the later predominantly decays via strong and/or electromagnetic interactions [14–16].

On the experimental side, a lot of progress has been made in the B_c meson properties and its decays [17–29]. It is believed that the LHCb is expected to produce 5×10^{10} events per year [29–31], which is around 10% of the total B meson data. This will provide a rich amount of information regarding B_c meson. At the same time, investigation of the nonleptonic B_s decays to excited state mesons provides an excellent opportunity to study D_s^{**} resonances, which are of the special interest for their masses being below the individual $D^{(*)}K$ thresholds [32]. Furthermore, the nonleptonic decays of B_c to orbitally excited $p-$wave $B_{(s)}^{**}$ mesons can help to understand the spectroscopy and mixing of $B_{(s)}$ excitation in light of heavy quark theory [32–40].

The developing theoretical and experimental aspects of the $B_c(B_s)$ meson physics motivate us to investigate the weak hadronic decays of $B_c(B_s)$ meson emitting a pseudoscalar (P) and an axial-vector (A) mesons in the final state. One can find several theoretical works based on the variety of quark models for the semileptonic and nonleptonic decays of $B_c(B_s)$ emitting $p-$wave mesons [14–16,41–73]. Semileptonic and nonleptonic decays of B_c into the $p-$wave and $d-$wave charmonium states are investigated in the perturbative QCD, the instantaneous Bethe–Salpeter and covariant light-front model frameworks, recently [57–61,63–65]. Similarly, the semileptonic and nonleptonic decays of the B_s meson into orbitally excited $p-$wave mesons have also been analyzed using the covariant light-front model and perturbative QCD framework [68,69]. Furthermore, in few of the approaches based on QCD sum rules and covariant light-front model, the HQET effects have been studied for the $B_c \to D^{**}/B_s^{**}$ transition form factors [62–64,67].

In the present work, we aim to employ the nonrelativistic quark model framework in heavy quark limit. The HQET provides an important tool to describe the spectroscopy and weak decays of hadrons involving heavy quark. Since, the mass of $b-$quark is much heavier than the QCD scale, the dynamics becomes much simpler in the light of heavy quark symmetries [5,7]. The HQET provides symmetry relations for the heavy meson decays; however, to incorporate HQET effects one needs a reliable model. Furthermore, one should be careful in implying the HQET for a system of two heavy quarks, such as B_c meson. In B_c meson, both $b-$ and $c-$quarks move around each other in a bound state. The kinetic-energy term, which is kept in the Lagrangian even at leading order, is different for both the quarks, thus breaking the flavor symmetry explicitly [14]. However, the heavy quark spin symmetry still remains,

[a] e-mail: dhir.rohit@gmail.com
[b] e-mail: nishu.vats@gmail.com (corresponding author)

Published online: 09 March 2022

because the spin–spin interaction between the quarks being proportional to $1/m_b m_c$ is expected to be small [14–16]. We employ the modified Isgur–Scora–Grinstein–Wise quark model (known as ISGW II quark model) [71,72] that not only satisfies HQET but also includes heavy quark symmetry constraints on the relations between the form factors, heavy-quark-symmetry-breaking, color magnetic interactions, relativistic corrections *etc*. In ISGW II model, the form factors are consistent with the constraints of heavy quark symmetry breaking at $\mathcal{O}(1/m_Q)$ to give more realistic physical form. We obtain $B_c(B_s) \to B^j_{(s)1}/D^j_{(s)1}$ transition form factors in ISGW II model, where $j = 1/2,\ 3/2$ represents $j - j$ coupled axial-vector $P_1^{1/2}$ and $P_1^{3/2}$ states with heavy quark spin $S_Q = 1/2,\ 3/2$, respectively, in the heavy quark symmetry [72]. We calculate the decay amplitudes and predict the branching ratios of nonleptonic $B_c(B_s) \to PA$ decays using the factorization hypothesis within the constraints of heavy quark symmetry. We made robust predictions for the decay modes involving $B_1/B_{s1}/D_1/D_{s1}$ mesons in the final states. For $B_c \to B_{(s)1}$ transitions, the mass of spectator $b-$quark is much larger than that of the decaying $c-$quark; the whole momentum is carried by the $b-$quark. Such decays are governed by the soft mechanism; therefore, the form factors in such case are insensitive to $1/m_Q$ corrections in the zero recoil limit. Thus, we obtain the branching ratios for $B_c \to B_{(s)1}P$ decays at maximum momentum transfer. However, we calculate the $B_c \to D_{(s)1}$ form factors away from the zero recoil but in consistency with ISGW II model in the HQS. For cohesion, we also calculate the $B_c(B_s) \to P$ transition form factors in ISGW II model framework [72].

The presentation of article goes as follows. We discuss the mass spectroscopy and mixing scheme in Sect. 2. Weak Hamiltonian, decay amplitudes, and form factors are discussed in Sect. 3. Numerical results and discussions are presented in Sect. 4, and last section contains summary and conclusions.

2 Mixing schemes

In the quark model, axial-vector mesons can exist in two types of spectroscopic states, *i.e.*, ${}^3P_1$ ($J^{PC} = 1^{++}$) and ${}^1P_1$ ($J^{PC} = 1^{+-}$). The physical states are expected to be a mixture of ${}^3P_1$ and ${}^1P_1$ states. However, the nonstrange and uncharmed mesons diagonal ${}^3P_1$ and ${}^1P_1$ systems cannot mix due to opposite C-parity. Experimentally [40], there exists ${}^3P_1$ multiplet with isovector $a_1(1.230)$ [1] and four isoscalars $f_1(1.285)$, $f_1(1.420)$, $f_1'(1.512)$, and $\chi_{c1}(3.511)$; and ${}^1P_1$ multiplet, isovector $b_1(1.229)$ and three isoscalars $h_1(1.170)$, $h_1'(1.380)$, and $h_{c1}(3.526)$, where spin and parity of the $h_{c1}(3.526)$ and C-parity of $h_1'(1.380)$ are yet to be confirmed. Similar to $\eta - \eta'$ mixing, flavor-singlet and flavor-octet axial-vector states can mix.

The strange and charmed axial-vector mesons are most likely a mixture of $|{}^3P_1\rangle \equiv A$ and $|{}^1P_1\rangle \equiv A'$ states, since there is no quantum number forbidding such mixing. For strange partners of A ($J^{PC} = 1^{++}$) and A' ($J^{PC} = 1^{+-}$) states, *i.e.*, K_{1A} and $K_{1A'}$ mesons:

$$\begin{aligned} K_1(1.270) &= K_{1A}\sin\theta_1 + K_{1A'}\cos\theta_1, \\ \underline{K}_1(1.400) &= K_{1A}\cos\theta_1 - K_{1A'}\sin\theta_1. \end{aligned} \tag{1}$$

The mixing of these states is not well determined due to the poor experimental data [40,70,74]. Nevertheless, several phenomenological and theoretical analyses [75,76] show that the mixing angles $\pm 37°,\ \pm 58°$ are possible; however, value $\sim 37°$ is preferred over $\sim 58°$. Thus, we use $\theta_1 = -(37 \pm 3)°$ in our calculations. Similarly, the mixing of charmed and strange charmed states can be given by

$$\begin{aligned} D_1(2.427) &= D_{1A}\sin\theta_{D_1} + D_{1A'}\cos\theta_{D_1}, \\ \underline{D}_1(2.422) &= D_{1A}\cos\theta_{D_1} - D_{1A'}\sin\theta_{D_1}. \end{aligned} \tag{2}$$

For the charmed and strange charmed states, in the infinite heavy quark mass limit, the spin of the heavy quark S_Q decouples from the light quark degrees of freedom [9], such that the heavy quark spin S_Q and the total angular momentum of the light antiquark can be used as good quantum numbers, separately. Therefore, the mass eigenstates ${}^3P_1$ and ${}^1P_1$ can be conveniently expressed as a mixture of $P_1^{3/2}$ and $P_1^{1/2}$ with $J^P = 1^+$ states in the heavy quark limit and vice versa, as follows:

$$\begin{pmatrix} |{}^3P_1\rangle \\ |{}^1P_1\rangle \end{pmatrix} = \begin{pmatrix} \sqrt{\frac{2}{3}} & \sqrt{\frac{1}{3}} \\ -\sqrt{\frac{1}{3}} & \sqrt{\frac{2}{3}} \end{pmatrix} \begin{pmatrix} |1^+,\ j = \frac{1}{2}\rangle \\ |1^+,\ j = \frac{3}{2}\rangle \end{pmatrix}. \tag{3}$$

The mixing angle θ_A from (2) can be defined as,

$$\theta_{D_1} = \theta_i + 35.26° \,. \tag{4}$$

where θ_i is defined in mixing of $j = 1/2$ and $j = 3/2$ states. Thus, the states $D_1(2.427)$ and $\underline{D}_1(2.422)$ can be identified as $P_1^{1/2}$ and $P_1^{3/2}$, respectively. However, beyond the heavy quark limit, there is a mixing between $P_1^{1/2}$ and $P_1^{3/2}$ given by

$$D_1(2.427) = D_1^{3/2}\sin\theta_1 + D_1^{1/2}\cos\theta_1,$$

[1] Numerical values given in the bracket represent the masses (in GeV) of the individual mesons.

$$\underline{D}_1(2.422) = D_1^{3/2}\cos\theta_1 - D_1^{1/2}\sin\theta_1. \tag{5}$$

For the strange charmed axial-vector mesons,

$$\begin{aligned} D_{s1}(2.460) &= D_{s1}^{3/2}\sin\theta_2 + D_{s1}^{1/2}\cos\theta_2, \\ \underline{D}_{s1}(2.535) &= D_{s1}^{3/2}\cos\theta_2 - D_{s1}^{1/2}\sin\theta_2. \end{aligned} \tag{6}$$

A detailed analysis by Belle [77] yields the mixing angle $\theta_1 = -(5.7 \pm 2.9)^\circ$, while the quark potential model [32,78,79] determines $\theta_2 \approx -7^\circ$; however, we use $\theta_2 = \theta_1$ in our calculations.

Since the quark model analysis has been quite successful in explaining the mixing of strange and charmed states. Therefore, for b-flavored mesons we use the following:

$$\begin{aligned} B_1(5.710) &= B_1^{3/2}\sin\theta_3 + B_1^{1/2}\cos\theta_3, \\ \underline{B}_1(5.726) &= B_1^{3/2}\cos\theta_3 - B_1^{1/2}\sin\theta_3, \end{aligned} \tag{7}$$

and

$$\begin{aligned} B_{s1}(5.820) &= B_{s1}^{3/2}\sin\theta_4 + B_{s1}^{1/2}\cos\theta_4, \\ \underline{B}_{s1}(5.830) &= B_{s1}^{3/2}\cos\theta_4 - B_{s1}^{1/2}\sin\theta_4, \end{aligned} \tag{8}$$

For the bottom states, we have taken masses from the review of particle physics [40]. Here also, in the light of review of literature that suggest wide range of mixing angles [32] and recent calculations [80], we use $\theta_3 = (18.2 \pm 3.5)^\circ$ and $\theta_4 = (4.1 \pm 1.5)^\circ$. For η and η' pseudoscalar states, we use

$$\begin{aligned} \eta(0.547) &= \tfrac{1}{\sqrt{2}}(u\bar{u} + d\bar{d})\sin\phi_P - (s\bar{s})\cos\phi_P, \\ \eta'(0.958) &= \tfrac{1}{\sqrt{2}}(u\bar{u} + d\bar{d})\cos\phi_P + (s\bar{s})\sin\phi_P, \end{aligned} \tag{9}$$

where $\phi_P = \theta_{ideal} - \theta_{physical}$, and $\theta_{physical} = -(14.1 \pm 2.8)^\circ$ [40]. η_c is taken as $\eta_c(2.979) = (c\bar{c})$.

3 Methodology

3.1 Weak Hamiltonian

For bottom-changing ($\Delta b = 1$) decays, the weak Hamiltonian involves the bottom-changing current,

$$J_\mu = (\bar{c}b)V_{cb} + (\bar{u}b)V_{ub}, \tag{10}$$

where $(\bar{q}_i q_j) \equiv \bar{q}_i\gamma_\mu(1-\gamma_5)q_j$ denotes the weak V-A current and V_{ij} are CKM elements [40]. QCD-modified weak Hamiltonian is then given below [3–5]:

a. for the decays involving $b \to c$ transition,

$$\begin{aligned} H_W = \frac{G_F}{\sqrt{2}}\big\{ & V_{cb}V_{ud}^*[a_1(\bar{c}b)(\bar{d}u) + a_2(\bar{d}b)(\bar{c}u)] + V_{cb}V_{cs}^*[a_1(\bar{c}b)(\bar{s}c) + a_2(\bar{s}b)(\bar{c}c)] \\ & + V_{cb}V_{us}^*[a_1(\bar{c}b)(\bar{s}u) + a_2(\bar{s}b)(\bar{c}u)] + V_{cb}V_{cd}^*[a_1(\bar{c}b)(\bar{d}c) + a_2(\bar{d}b)(\bar{c}c)]\big\}, \end{aligned} \tag{11}$$

b. for the decays involving $b \to u$ transition,

$$\begin{aligned} H_W = \frac{G_F}{\sqrt{2}}\big\{ & V_{ub}V_{cs}^*[a_1(\bar{u}b)(\bar{s}c) + a_2(\bar{s}b)(\bar{u}c)] + V_{ub}V_{ud}^*[a_1(\bar{u}b)(\bar{d}u) + a_2(\bar{d}b)(\bar{u}u)] \\ & + V_{ub}V_{us}^*[a_1(\bar{u}b)(\bar{s}u) + a_2(\bar{s}b)(\bar{u}u)] + V_{ub}V_{cd}^*[a_1(\bar{u}b)(\bar{d}c) + a_2(\bar{d}b)(\bar{u}c)]\big\} \end{aligned} \tag{12}$$

c. for the decays involving the $c \to s$ transition,

$$H_W = \frac{G_F}{\sqrt{2}}\big\{V_{ud}V_{cs}^*[a_1(\bar{u}d)(\bar{s}c) + a_2(\bar{u}c)(\bar{s}d)]\big\}. \tag{13}$$

By factorizing matrix elements of the four-quark operator contained in the effective Hamiltonian (11), (12), and (13), one can distinguish three classes of decays [1,3,4]:

1. The first class (Class I) contains those decays which can be generated from the color singlet current and the decay amplitudes are proportional to a_1, where $a_1(\mu) = c_1(\mu) + \frac{1}{N_c}c_2(\mu)$, and N_c is the number of colors.

2. The second class (Class II) of transitions consist of those decays, which can be generated from the neutral current. The decay amplitude in this class is proportional to a_2, *i.e.*, for the color-suppressed modes, $a_2(\mu) = c_2(\mu) + \frac{1}{N_c} c_1(\mu)$.
3. The third class (Class III) of decay modes can be generated from the interference of color singlet and color neutral currents, *i.e.*, the a_1 and a_2 amplitudes interfere.

However, we follow the convention of large N_c limit to fix the QCD coefficients $a_1 \approx c_1$ and $a_2 \approx c_2$, [1,3,4] and use the following numerical values:

$$\begin{aligned} c_1(\mu) &= (1.26 \pm 0.10),\ c_2(\mu) = -(0.51 \pm 0.10)\ \text{ at }\ \mu \approx m_c^2. \\ c_1(\mu) &= (1.12 \pm 0.20),\ c_2(\mu) = -(0.26 \pm 0.15)\ \text{ at }\ \mu \approx m_b^2. \end{aligned} \tag{14}$$

We wish to remark here that for the charm-changing (bottom conserving) decays, the phenomenological parameterization of a_1 and a_2 from experimental charm decays suggests that the large N_c limit can be considered as theoretical benchmark for charm meson decays [81]. However, for bottom-changing decays phenomenological analyses [82] suggest a varying magnitude of Wilson coefficients a_1 and a_2 (as well as subleading contribution to $1/N_c$ term), which can be included by allowing certain range in these coefficients as in (14). It may be noted that the decay amplitudes can be expressed as factorizable contributions multiplied by corresponding a_i's that are (renormalization) scale and process independent. As we have mentioned earlier, $B_c(B_s)$ decays either proceed only via tree diagrams or are tree-dominated; therefore, we neglect the expected small nonfactorizable and penguin contributions in our formalism.

3.2 Decay amplitudes

The decay rate formula[2] for $B \to PA$ decays is given by

$$\Gamma(B \to PA) = \frac{p_c^3}{8\pi m_A^2} |A(B \to PA)|^2 , \tag{15}$$

where p_c is the magnitude of the three-momentum of a final-state particle in the rest frame of $B \equiv \{B_c,\ B_s\}$ meson and m_A denotes the mass of axial-vector meson.

The factorization scheme expresses the decay amplitudes as a product of the matrix elements of weak currents (up to the weak scale factor of $\frac{G_F}{\sqrt{2}} \times$ CKM elements $\times$ QCD factor) as

$$\langle PA|\, H_w\, |B\rangle \sim \langle P|\, J^\mu\, |0\rangle\, \langle A|\, J_\mu\, |B\rangle + \langle A|\, J^\mu\, |0\rangle\, \langle P|\, J_\mu\, |B\rangle , \tag{16}$$

$$\left\langle PA^{'}\right|\, H_w\, |B\rangle \sim \langle P|\, J^\mu\, |0\rangle \left\langle A^{'}\right|\, J_\mu\, |B\rangle + \left\langle A^{'}\right|\, J^\mu\, |0\rangle\, \langle P|\, J_\mu\, |B\rangle . \tag{17}$$

Using Lorentz invariance, matrix elements of the $B \to A$ transitions are given below [72]:

$$\begin{aligned} \langle A^{1/2}(P_A)|V_\mu|B(P_B)\rangle &= i[\ell_{\frac{1}{2}}(q^2)\varepsilon_\mu^* + c_{+\frac{1}{2}}(q^2)(\varepsilon^* \cdot P_B)(P_B + P_A)_\mu \\ &\quad + c_{-\frac{1}{2}}(q^2)(\varepsilon^* \cdot P_B)(P_B - P_A)_\mu], \\ \langle A^{1/2}(P_A)|A_\mu|B(P_B)\rangle &= -q_{\frac{1}{2}}(q^2)\epsilon_{\mu\nu\rho\sigma}\varepsilon^{*\nu}(P_B + P_A)^\rho (P_B - P_A)^\sigma, \\ \langle A^{3/2}(P_A)|V_\mu|B(P_B)\rangle &= i[\ell_{\frac{3}{2}}(q^2)\varepsilon_\mu^* + c_{+\frac{3}{2}}(q^2)(\varepsilon^* \cdot P_B)(P_B + P_A)_\mu \\ &\quad + c_{-\frac{3}{2}}(q^2)(\varepsilon^* \cdot P_B)(P_B - P_A)_\mu], \\ \langle A^{3/2}(P_A)|A_\mu|B(P_B)\rangle &= -q_{\frac{3}{2}}(q^2)\epsilon_{\mu\nu\rho\sigma}\varepsilon^{*\nu}(P_B + P_A)^\rho (P_B - P_A)^\sigma. \end{aligned} \tag{18}$$

It may be noted that $B_c(B_s) \to A$ transition form factors in ISGW II framework can be related to BSW-type form factor [83] notations, *i.e.*, A, $V_{0,1,2}$ through the following relations

$$\begin{aligned} A(q^2) &= -q(q^2)(m_B + m_A); \\ V_1(q^2) &= l(q^2)/(m_B + m_A); \\ V_2(q^2) &= -c_+(q^2)(m_B + m_A); \\ V_0^{3/2}(q^2) &= \frac{1}{(2m_A)}[(m_B + m_A)V_1(q^2) - (m_B - m_A)V_2(q^2) - q^2 c_-(q^2)]. \end{aligned} \tag{19}$$

The decay constants of a pseudoscalar meson and an axial-vector meson state are given by the relations [72],

$$\langle 0|\, J_\mu\, |P\rangle = -i f_P k_\mu, \tag{20}$$

[2] The decay width formula is modified when the polarization of axial-vector meson appearing in square of the amplitude as $\epsilon \cdot p_B$ is replaced by $p_c(m_B/m_A)$.

$$\langle 0|\, J_\mu \,|A^{1/2}\rangle = \varepsilon_\mu^* m_{A^{1/2}} f_{A^{1/2}}, \tag{21}$$

$$\langle 0|\, J_\mu \,|A^{3/2}\rangle = \varepsilon_\mu^* m_{A^{3/2}} f_{A^{3/2}}. \tag{22}$$

Sandwiching the weak Hamiltonian (11), (12), and (13) between the initial and final states, the factorizable decay amplitudes for various $B_c(B_s) \to PA$ decay modes can be obtained (with common $\frac{G_F}{\sqrt{2}}\times$CKM factors) as:

$$\begin{aligned}
A(B \to PA) = -2(\varepsilon^* \cdot p_B)\Big\{ & a_1 f_P\Big[V_0^{BA^{3/2}}(m_P^2) m_{A^{3/2}} \sin\theta + V_0^{BA^{1/2}}(m_P^2) m_{A^{1/2}} \cos\theta\Big] \\
& + a_2\Big[F_1^{BP}(m_{A^{3/2}}^2) m_{A^{3/2}} f_{A^{3/2}} \sin\theta + F_1^{BP}(m_{A^{1/2}}^2) m_{A^{1/2}} f_{A^{1/2}} \cos\theta\Big]\Big\}, \\
A(B \to PA') = -2(\varepsilon^* \cdot p_B)\Big\{ & a_1 f_P\Big[V_0^{BA^{3/2}}(m_P^2) m_{A^{3/2}} \cos\theta - V_0^{BA^{1/2}}(m_P^2) m_{A^{1/2}} \sin\theta\Big] \\
& + a_2\Big[F_1^{BP}(m_{A^{3/2}}^2) m_{A^{3/2}} f_{A^{3/2}} \cos\theta - F_1^{BP}(m_{A^{1/2}}^2) m_{A^{1/2}} f_{A^{1/2}} \sin\theta\Big]\Big\}.
\end{aligned} \tag{23}$$

3.3 Form factors in the heavy quark symmetry

The ISGW II quark model incorporates HQS constraints and employs HQET for the systematical treatment of the perturbative QCD corrections and $1/m_Q$ expansion. Moreover, the ISGW II model can be an excellent approximation for the $b\bar{c}$ system. The B_c meson can reasonably be treated as nonrelativistic system, and the matrix elements can be accurately determined by simple wave function overlap integrals. Aforementioned, for excited p-wave heavy quark systems, heavy quark symmetry yields the spin parity states, ${}^3P_1$ and ${}^1P_1$, as the $j-j$ coupled states with $s_\ell^{\pi_\ell} = \frac{3}{2}^+$ and $\frac{1}{2}^+$. The form factors $\ell_{\frac{3}{2}}$, $c_{+\frac{3}{2}}$, $c_{-\frac{3}{2}}$, and $q_{\frac{3}{2}}$ replace the ℓ, c_+, c_-, and q for the $s_\ell^{\pi_\ell} = \frac{3}{2}^+$ state with $J^P = 1^+$ (see equations (B26) and (B27) of ISGW II [72]), and a parallel set $\ell_{\frac{1}{2}}$, $c_{+\frac{1}{2}}$, $c_{-\frac{1}{2}}$, and $q_{\frac{1}{2}}$ for the $s_\ell^{\pi_\ell} = \frac{1}{2}^+$ state with $J^P = 1^+$, then [72]:

$$\ell_{\frac{3}{2}} = -\frac{2\tilde{m}_B\beta_B}{\sqrt{3}}\left\{\frac{1}{m_q} + \frac{\tilde{m}_X m_d(\tilde{w}-1)}{2\beta_B^2}\left(\frac{\tilde{w}+1}{2m_q} - \frac{m_d\beta_B^2}{2\mu_-\tilde{m}_X\beta_{BX}^2}\right)\right\} F_5^{(\ell_{\frac{3}{2}})} \tag{24}$$

$$c_{+\frac{3}{2}} + c_{-\frac{3}{2}} = -\frac{\sqrt{3}m_d}{2\beta_B\tilde{m}_B}\left[1 - \frac{m_d}{3m_q} - \frac{m_d\beta_B^2}{3\beta_{BX}^2}\left(\frac{1}{2\mu_-} - \frac{1}{\mu_+}\right)\right] F_5^{(c_{+\frac{3}{2}}+c_{-\frac{3}{2}})} \tag{25}$$

$$c_{+\frac{3}{2}} - c_{-\frac{3}{2}} = -\frac{m_d}{2\sqrt{3}\beta_B\tilde{m}_X}\left[\frac{(2-\tilde{w})\tilde{m}_X}{m_q} + \frac{m_d\beta_B^2}{\beta_{BX}^2}\left(\frac{1}{2\mu_-} - \frac{1}{\mu_+}\right)\right] F_5^{(c_{+\frac{3}{2}}-c_{-\frac{3}{2}})} \tag{26}$$

$$q_{\frac{3}{2}} = -\frac{1}{2\sqrt{3}}\left\{\frac{1+\tilde{w}}{2} + \frac{\beta_B^2\tilde{m}_B}{2m_d m_q m_b}\right\}\frac{m_d}{\beta_b\tilde{m}_X} F_5^{(q_{\frac{3}{2}})} \tag{27}$$

and

$$\ell_{\frac{1}{2}} = \sqrt{\frac{2}{3}}\tilde{m}_B\beta_B\left\{\frac{1}{2m_q} - \frac{3}{2m_b} + \frac{m_d\tilde{m}_X(\tilde{w}-1)}{\beta_B^2}\left[\frac{1}{m_q} - \frac{m_d\beta_B^2}{2\mu_-\tilde{m}_X\beta_{BX}^2}\right]\right\} F_5^{(\ell_{\frac{1}{2}})} \tag{28}$$

$$c_{+\frac{1}{2}} + c_{-\frac{1}{2}} = \frac{m_d^2\beta_X^2}{\sqrt{6}\tilde{m}_B m_q\beta_B\beta_{BX}^2} F_5^{(c_{+\frac{1}{2}}+c_{-\frac{1}{2}})} \tag{29}$$

$$c_{+\frac{1}{2}} - c_{-\frac{1}{2}} = -\sqrt{\frac{2}{3}}\frac{m_d}{\tilde{m}_X\beta_B}\left[1 + \frac{m_d\beta_X^2}{2m_q\beta_{BX}^2}\right] F_5^{(c_{+\frac{1}{2}}-c_{-\frac{1}{2}})} \tag{30}$$

$$q_{\frac{1}{2}} = \sqrt{\frac{1}{6}}\left\{1 - \frac{\beta_B^2\tilde{m}_B}{4m_d m_q m_b}\right\}\frac{m_d}{\beta_B\tilde{m}_X} F_5^{(q_{\frac{1}{2}})}. \tag{31}$$

where

$$F_5^{(l_{\frac{3}{2}(\frac{1}{2})})} = F_5\left(\frac{\bar{m}_B}{\tilde{m}_B}\right)^{1/2}\left(\frac{\bar{m}_A}{\tilde{m}_A}\right)^{1/2},$$

$$F_5^{(c_{+\frac{3}{2}(\frac{1}{2})} + c_{-\frac{3}{2}(\frac{1}{2})})} = F_5\left(\frac{\bar{m}_B}{\tilde{m}_B}\right)^{-3/2}\left(\frac{\bar{m}_A}{\tilde{m}_A}\right)^{1/2},$$

Table 1 The parameter β for s-wave and p-wave mesons in the ISGW II quark model

Quark content	$u\bar{d}$	$u\bar{s}$	$s\bar{s}$	$c\bar{u}$	$c\bar{s}$	$u\bar{b}$	$s\bar{b}$	$c\bar{c}$	$b\bar{c}$
β_s(GeV)	0.41	0.44	0.53	0.45	0.56	0.43	0.54	0.88	0.92
β_p(GeV)	0.28	0.30	0.33	0.33	0.38	0.35	0.41	0.52	0.60

$$F_5^{(c_{+\frac{3}{2}(\frac{1}{2})} - c_{-\frac{3}{2}(\frac{1}{2})})} = F_5 \left(\frac{\bar{m}_B}{\tilde{m}_B}\right)^{-1/2} \left(\frac{\bar{m}_A}{\tilde{m}_A}\right)^{-1/2}. \tag{32}$$

The $t(\equiv q^2)$dependence is given by:

$$\tilde{\omega} - 1 = \frac{t_m - t}{2\bar{m}_B \bar{m}_A}, \tag{33}$$

and

$$F_5 = \left(\frac{\tilde{m}_A}{\tilde{m}_B}\right)^{1/2} \left(\frac{\beta_B \beta_A}{B_{BA}}\right)^{5/2} \left[1 + \frac{1}{18} h^2 (t_m - t)\right]^{-3}, \tag{34}$$

where

$$h^2 = \frac{3}{4m_c m_q} + \frac{3m_d^2}{2\bar{m}_B \bar{m}_A \beta_{BA}^2} + \frac{1}{\bar{m}_B \bar{m}_A} \left(\frac{16}{33 - 2n_f}\right) \ln\left[\frac{\alpha_S(\mu_{QM})}{\alpha_S(m_q)}\right],$$

with

$$\beta_{BA}^2 = \frac{1}{2}\left(\beta_B^2 + \beta_A^2\right), \tag{35}$$

and

$$\mu_{\pm} = \left(\frac{1}{m_q} \pm \frac{1}{m_b}\right)^{-1}.$$

$\tilde{m}$ and $\bar{m}$ denote the sum of the mesons constituent quarks masses and the hyperfine-averaged physical masses, respectively. The maximum momentum transfer is given by $t_m = (m_B - m_A)^2$, μ_{QM} is the quark model scale, while n_f is the number of active flavors. The subscript q depends upon the quark currents, $\bar{q}\gamma_\mu b$ and $\bar{q}\gamma_\mu\gamma_5 b$, appearing in different transitions. The values of the β-parameter used for different s-wave and p-wave mesons are given in Table 1. It is well known that the ISGW model, like most of the theoretical models, suffers from typical uncertainties associated with quark model parameters, mainly quark masses. The form factors are sensitive to the quark mass variation; therefore, we allow variation in quark masses yielding uncertainties in the form factors. We use the following constituent quark masses (in GeV):

$$m_u = m_d = (0.33 \pm 0.03),\ m_s = (0.50 \pm 0.03),\ m_c = (1.67 \pm 0.03),\ \text{and}\ m_b = (5.10 \pm 0.03),$$

to calculate the form factors for $B_c(B_s) \to B^j_{(s)1}/D^j_{(s)1}$ transitions. The obtained form factors are given in Table 2. Following the procedure given in [48,72], we obtained the $B_c(B_s) \to P$ form factors in ISGW II as shown in Table 3.

4 Numerical results and discussions

In the present work, we have obtained the branching ratios (which are expected to be tree-dominated) of B_c and B_s mesons for the various decay modes in CKM-favored and CKM-suppressed modes involving $D_1^{(\prime)}$ and $D_{s1}^{(\prime)}$ mesons in the final state. We have used the following decay constants [40,84,85] For the pseudoscalar mesons: $f_\pi = (130.2 \pm 0.8)$ MeV, $f_K = (155.7 \pm 0.3)$ MeV, $f_D = (212.6 \pm 0.7)$ MeV, $f_{D_s} = 249.9 \pm 0.5$ MeV, $f_\eta = (133.0 \pm 0.4)$ MeV, $f_{\eta'} = (126.0 \pm 0.4)$ MeV, and $f_{\eta_c} = (398.0 \pm 1.0)$ MeV. The numerical values of the axial-vector meson decay constants used are [86,87]: $f_{D_{1A}} = -(177 \pm 36)$ MeV, $f_{D'_{1A}} = (59.6 \pm 9.6)$ MeV, $f_{D_{s1A}} = -(159 \pm 34)$ MeV, $f_{D'_{s1A}} = (42.2 \pm 7.4)$ MeV, and $f_{\chi_{c1}} \approx -207$ MeV. Taking in to account all the uncertainties from quark-masses, CKM factors (we use numerical values from [40]), mixing angles, form factors, decay constants, *etc.*, we obtained the results for charm-changing and bottom-conserving modes based on the heavy quark symmetry constraints using the ISGW II quark model as shown in Table 4. The calculated branching ratios for CKM-favored and CKM-suppressed bottom-changing modes are given in Tables 5, 6, 7, 8, 9, and 10. The following are our observations.

Table 2 Form factors of $B_q \to D_1^{1/2}, D_1^{3/2}$ transitions at $q^2 = 0$ and $B_c \to B_{(s)1}^{1/2}, B_{(s)1}^{3/2}$ transitions at q^2 = maximum in the ISGW II quark model using HQS

Transition	ℓ	c_+	c_-
ISGW II with HQS Constraints			
$B_s \to D_{s1}^{1/2}$	-0.27 ± 0.02	-0.11 ± 0.01	0.11 ± 0.01
$B_s \to D_{s1}^{3/2}$	-1.11 ± 0.03	-0.16 ± 0.01	-0.091 ± 0.006
$B_c \to D_1^{1/2}$	0.90 ± 0.07	-0.047 ± 0.001	0.062 ± 0.002
$B_c \to D_1^{3/2}$	-2.47 ± 0.19	-0.050 ± 0.001	-0.052 ± 0.001
$B_c \to D_{s1}^{1/2}$	0.86 ± 0.05	-0.064 ± 0.001	0.082 ± 0.002
$B_c \to D_{s1}^{3/2}$	-2.60 ± 0.14	-0.080 ± 0.001	-0.072 ± 0.001
$B_c \to B_1^{1/2}$	5.4 ± 1.0	0.124 ± 0.022	-0.49 ± 0.06
$B_c \to B_1^{3/2}$	1.95 ± 0.19	0.28 ± 0.04	0.48 ± 0.11
$B_c \to B_{s1}^{1/2}$	20.4 ± 2.6	0.43 ± 0.06	-1.61 ± 0.15
$B_c \to B_{s1}^{3/2}$	0.6 ± 0.6	0.88 ± 0.11	1.74 ± 0.26

Table 3 Form factors of $B_q \to P$ transitions at $q^2 = 0$ in the ISGW II quark model

Transition	f_+	f_-
ISGW II		
$B_s \to K$	1.3 ± 0.6	-1.2 ± 0.6
$B_s \to \eta$	0.47 ± 0.07	-0.41 ± 0.07
$B_s \to \eta'$	0.72 ± 0.08	-0.63 ± 0.06
$B_s \to D_s$	0.73 ± 0.01	-0.39 ± 0.01
$B_c \to D$	0.35 ± 0.10	-0.32 ± 0.10
$B_c \to D_s$	0.32 ± 0.02	-0.28 ± 0.02
$B_c \to \eta_c$	0.64 ± 0.01	-0.38 ± 0.01

Table 4 Branching ratios of $B_c \to PA$ decays in charm-changing decay modes

Decays	Branching ratios
$\Delta C = -1, \Delta S = -1$	
$B_c^+ \to \pi^+ B_{s1}^0$	$(6.9 \pm 2.0) \times 10^{-2}$
$B_c^+ \to \pi^+ B_{s1}^{0'}$	$(1.4 \pm 0.7) \times 10^{-3}$
$B_c^+ \to \bar{K}^0 B_1^+$	$(3.1 \pm 1.5) \times 10^{-4}$
$B_c^+ \to \bar{K}^0 B_1^{+'}$	$(2.0 \pm 1.2) \times 10^{-4}$
$\Delta C = -1, \Delta S = 0$	
$B_c^+ \to \pi^+ B_1^0$	$(5.8 \pm 2.0) \times 10^{-4}$
$B_c^+ \to \pi^+ B_1^{0'}$	$(1.0 \pm 0.5) \times 10^{-4}$
$B_c^+ \to \pi^0 B_1^+$	$(4.8 \pm 2.4) \times 10^{-5}$
$B_c^+ \to \pi^0 B_1^{+'}$	$(8.0 \pm 4.0) \times 10^{-6}$
$B_c^+ \to \eta B_1^+$	$(3.1 \pm 2.8) \times 10^{-8}$
$B_c^+ \to \eta B_1^{+'}$	$(1.0 \pm 0.9) \times 10^{-7}$
$\Delta C = -1, \Delta S = 1$	
$B_c^+ \to K^+ B_1^0$	$(5.5 \pm 2.0) \times 10^{-6}$
$B_c^+ \to K^+ B_1^{0'}$	$(3.3 \pm 1.5) \times 10^{-6}$
$B_c^+ \to K^0 B_1^+$	$(8.2 \pm 4.2) \times 10^{-7}$
$B_c^+ \to K^0 B_1^{+'}$	$(5.2 \pm 3.1) \times 10^{-7}$

Table 5 Branching ratios for $B_q \to PA$ decays in bottom-changing CKM-favored decay mode $\Delta b = 1$, $\Delta C = 1$, $\Delta S = 0$

Decays	Branching ratios
$\bar{B_s}^0 \to \pi^- D_{s1}^+$	$(1.4 \pm 0.6) \times 10^{-3}$
$\bar{B_s}^0 \to \pi^- D_{s1}^{+'}$	$(7.2 \pm 2.7) \times 10^{-3}$
$\bar{B_s}^0 \to K^0 D_1^0$	$(2.3 \pm 1.2) \times 10^{-3}$
$\bar{B_s}^0 \to K^0 D_1^{0'}$	$(0.9 \pm 0.5) \times 10^{-4}$
$B_c^- \to D^0 D_1^-$	$(1.2 \pm 0.8) \times 10^{-8}$
$B_c^- \to D^0 D_1^{-'}$	$(4.6 \pm 3.9) \times 10^{-4}$
$B_c^- \to D^- D_1^0$	$(1.0 \pm 0.6) \times 10^{-4}$
$B_c^- \to D^- D_1^{0'}$	$(3.7 \pm 1.9) \times 10^{-6}$

Table 6 Branching ratios for $B_q \to PA$ decays in bottom-changing CKM-favored decay mode $\Delta b = 1$, $\Delta C = 0$, $\Delta S = -1$

Decays	Branching ratios
$\bar{B_s}^0 \to D_s^- D_{s1}^+$	$(1.2 \pm 0.6) \times 10^{-3}$
$\bar{B_s}^0 \to D_s^- D_{s1}^{+'}$	$(1.0 \pm 0.4) \times 10^{-2}$
$\bar{B_s}^0 \to D_s^+ D_{s1}^-$	$(3.7 \pm 2.0) \times 10^{-3}$
$\bar{B_s}^0 \to D_s^+ D_{s1}^{-'}$	$(2.4 \pm 1.1) \times 10^{-4}$
$B_c^- \to \eta_c D_{s1}^-$	$(1.3 \pm 0.7) \times 10^{-3}$
$B_c^- \to \eta_c D_{s1}^{-'}$	$(2.8 \pm 2.5) \times 10^{-4}$
$B_c^- \to K^- \bar{D}_1^0$	$(0.8 \pm 0.4) \times 10^{-8}$
$B_c^- \to K^- \bar{D}_1^{0'}$	$(2.6 \pm 1.0) \times 10^{-6}$
$B_c^- \to \pi^0 D_{s1}^-$	$(1.5 \pm 1.4) \times 10^{-9}$
$B_c^- \to \pi^0 D_{s1}^{-'}$	$(7.0 \pm 5.0) \times 10^{-8}$
$B_c^- \to \eta D_{s1}^-$	$(1.0 \pm 0.6) \times 10^{-9}$
$B_c^- \to \eta D_{s1}^{-'}$	$(4.0 \pm 3.0) \times 10^{-8}$
$B_c^- \to \eta^{'} D_{s1}^-$	$(4.2 \pm 2.8) \times 10^{-10}$
$B_c^- \to \eta^{'} D_{s1}^{-'}$	$(2.9 \pm 2.5) \times 10^{-8}$

Table 7 Branching ratios for $B_q \to PA$ decays in bottom-changing CKM-suppressed decay mode $\Delta b = 1$, $\Delta C = 1$, $\Delta S = -1$

Decays	Branching ratios
$\bar{B_s}^0 \to K^- D_{s1}^+$	$(1.1 \pm 0.4) \times 10^{-4}$
$\bar{B_s}^0 \to K^- D_{s1}^{+'}$	$(5.2 \pm 2.0) \times 10^{-4}$
$\bar{B_s}^0 \to \eta D_1^0$	$(7.0 \pm 5.0) \times 10^{-6}$
$\bar{B_s}^0 \to \eta D_1^{0'}$	$(3.0 \pm 2.0) \times 10^{-7}$
$\bar{B_s}^0 \to \eta^{'} D_1^0$	$(2.0 \pm 1.6) \times 10^{-5}$
$\bar{B_s}^0 \to \eta^{'} D_1^{0'}$	$(7.0 \pm 5.5) \times 10^{-7}$
$B_c^- \to D^0 D_{s1}^-$	$(1.9 \pm 1.3) \times 10^{-7}$
$B_c^- \to D^0 D_{s1}^{-'}$	$(3.0 \pm 2.4) \times 10^{-5}$
$B_c^- \to D_s^- D_1^0$	$(3.8 \pm 3.0) \times 10^{-6}$
$B_c^- \to D_s^- D_1^{0'}$	$(1.4 \pm 1.0) \times 10^{-7}$

Table 8 Branching ratios for $B_q \to PA$ decays in bottom-changing CKM-suppressed decay mode $\Delta b = 1$, $\Delta C = 0$, $\Delta S = 0$

Decays	Branching ratios
$\bar{B_s}^0 \to D^- D_{s1}^+$	$(5.5 \pm 2.5) \times 10^{-5}$
$\bar{B_s}^0 \to D^- D_{s1}^{+'}$	$(4.4 \pm 1.6) \times 10^{-4}$
$\bar{B_s}^0 \to D_s^+ D_1^-$	$(2.6 \pm 1.3) \times 10^{-4}$
$\bar{B_s}^0 \to D_s^+ D_1^{-'}$	$(1.0 \pm 0.7) \times 10^{-5}$
$B_c^- \to \eta_c D_1^-$	$(8.1 \pm 4.0) \times 10^{-5}$
$B_c^- \to \eta_c D_1^{-'}$	$(1.1 \pm 0.8) \times 10^{-5}$
$B_c^- \to \pi^- \bar{D}_1^0$	$(1.2 \pm 0.7) \times 10^{-7}$
$B_c^- \to \pi^- \bar{D}_1^{0'}$	$(3.5 \pm 1.4) \times 10^{-5}$
$B_c^- \to \pi^0 D_1^-$	$(3.0 \pm 1.6) \times 10^{-9}$
$B_c^- \to \pi^0 D_1^{-'}$	$(1.1 \pm 0.8) \times 10^{-6}$
$B_c^- \to \eta D_1^-$	$(1.7 \pm 0.9) \times 10^{-9}$
$B_c^- \to \eta D_1^{-'}$	$(6.0 \pm 4.8) \times 10^{-7}$
$B_c^- \to \eta^{'} D_1^-$	$(0.7 \pm 0.4) \times 10^{-9}$
$B_c^- \to \eta^{'} D_1^{-'}$	$(3.4 \pm 3.0) \times 10^{-7}$

Table 9 Branching ratios for $B_q \to PA$ decays in bottom-changing CKM-doubly-suppressed decay mode $\Delta b = 1$, $\Delta C = -1$, $\Delta S = 0$

Decays	Branching ratios
$\bar{B_s}^0 \to K^+ D_1^-$	$(1.7 \pm 1.4) \times 10^{-5}$
$\bar{B_s}^0 \to K^+ D_1^{-'}$	$(6.0 \pm 5.0) \times 10^{-7}$
$\bar{B_s}^0 \to K^0 \bar{D}_1^0$	$(1.0 \pm 0.6) \times 10^{-6}$
$\bar{B_s}^0 \to K^0 \bar{D}_1^{0'}$	$(4.0 \pm 2.0) \times 10^{-8}$
$B_c^- \to D^- \bar{D}_1^0$	$(5.0 \pm 3.5) \times 10^{-8}$
$B_c^- \to D^- \bar{D}_1^{0'}$	$(3.1 \pm 1.2) \times 10^{-6}$
$B_c^- \to \bar{D}^0 D_1^-$	$(8.0 \pm 5.5) \times 10^{-7}$
$B_c^- \to \bar{D}^0 D_1^{-'}$	$(6.2 \pm 5.6) \times 10^{-8}$

Table 10 Branching ratios for $B_q \to PA$ decays in bottom-changing CKM-doubly-suppressed decay mode $\Delta b = 1$, $\Delta C = -1$, $\Delta S = -1$

Decays	Branching ratios
$\bar{B_s}^0 \to K^+ D_{s1}^-$	$(2.5 \pm 1.5) \times 10^{-4}$
$\bar{B_s}^0 \to K^+ D_{s1}^{-'}$	$(1.7 \pm 1.3) \times 10^{-5}$
$\bar{B_s}^0 \to \eta \bar{D}_1^0$	$(1.1 \pm 0.5) \times 10^{-6}$
$\bar{B_s}^0 \to \eta \bar{D}_1^{0'}$	$(4.5 \pm 1.5) \times 10^{-8}$
$\bar{B_s}^0 \to \eta^{'} \bar{D}_1^0$	$(3.1 \pm 2.6) \times 10^{-6}$
$\bar{B_s}^0 \to \eta^{'} \bar{D}_1^{0'}$	$(1.2 \pm 0.9) \times 10^{-7}$
$B_c^- \to D_s^- \bar{D}_1^0$	$(6.0 \pm 1.8) \times 10^{-7}$
$B_c^- \to D_s^- \bar{D}_1^{0'}$	$(8.2 \pm 3.2) \times 10^{-5}$
$B_c^- \to \bar{D}^0 D_{s1}^-$	$(1.3 \pm 0.3) \times 10^{-5}$
$B_c^- \to \bar{D}^0 D_{s1}^{-'}$	$(1.7 \pm 1.5) \times 10^{-6}$

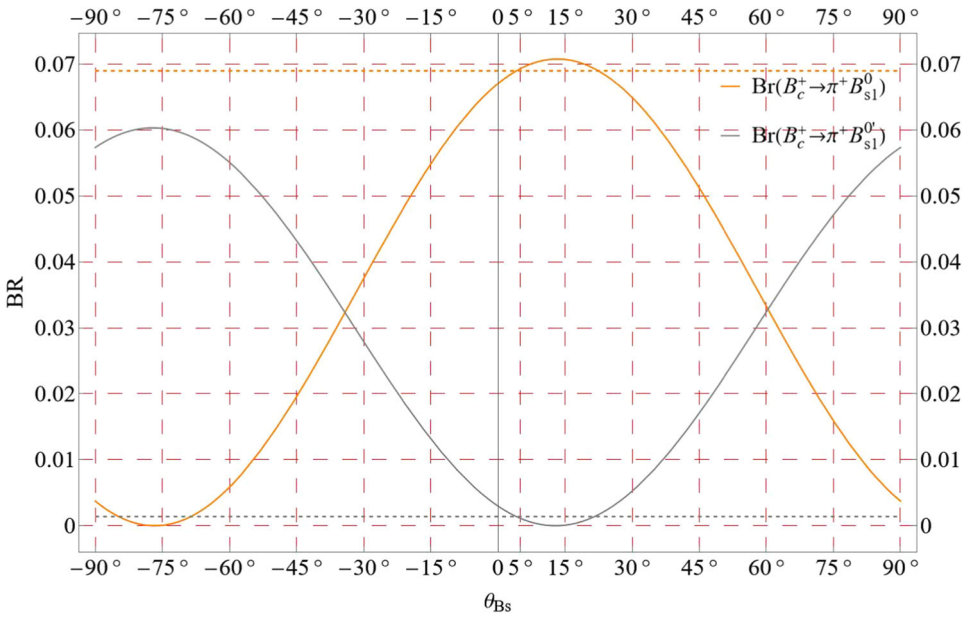

Fig. 1 Dependence of the branching ratios on mixing angle θ_{B_s}. Theoretical branching ratios are shown as dashed lines: orange and gray for $B_c^+ \to \pi^+ B_{s1}^0$ and $B_c^+ \to \pi^+ B_{s1}^{0'}$, respectively

4.1 Bottom-conserving and charm-changing decay modes

In this subsection, we give the results for B_c meson decaying to B_1 and B_{s1} mesons; the form factors used to calculate the branching ratios are given in Table 4. We list our major findings as:

i. The most dominant CKM and color-favored (Class I) decay, $B_c^+ \to \pi^+ B_{s1}^0$ has branching ratio $(6.9 \pm 2.0) \times 10^{-2}$. However, the branching ratio of $B_c^+ \to \pi^+ B_{s1}^{0'}$ decay is smaller, roughly, by an order of magnitude owing to the mixing scheme. Usually, the $c \to d/s$ decays are expected to be kinematically suppressed; however, the large CKM factor enhance the branching ratios of these decays. We wish to point out that for bottom-conserving ($B_c \to B_{(s)}$) decays, the mass of the spectator $b-$quark is much greater than that of the decaying $c-$quark, the energy released in the decay process is much smaller than m_b, and the whole momentum is carried by the $b-$quark. Thus, the transition form factors in such case are best understood at maximum momentum transfer between initial and final states. Further, it is well established that form factors in such case are insensitive to $1/m_Q$ corrections in the zero recoil limit [14]. Therefore, we predict the branching ratios of $B_c \to B_{(s)} P$ decays at maximum momentum transfer in heavy quark limit. The color-suppressed (Class II) modes have: $B(B_c^+ \to \bar{K}^0 B_1^{+'}) = (3.1 \pm 1.5) \times 10^{-4}$ and $B(B_c^+ \to \bar{K}^0 B_1^+) = (2.0 \pm 1.2) \times 10^{-4}$. The $\theta_{B_{(s)}}$ dependence of the branching ratios for these decays is shown in Figs. 1 and 2. The suppressed branching ratio for $B_c^+ \to \bar{K}^0 B_1^+$ w.r.t variation of θ could be attributed mainly to relative negative sign between $P_1^{3/2}$ and $P_1^{1/2}$ amplitudes, smaller form factors and color suppression. Thus, the observation of such decays can be useful to understand the mixing of heavy flavor axial-vector mesons in HQS and fix the relative signs and magnitudes of the form factors involved. It may be noted that the large uncertainties, nearly $\mathcal{O}(50\%)$, appearing in the branching ratios for some of the decay modes are mainly propagating from the form factors, QCD coefficients and mixing angles.

ii. Dominant branching ratios of bottom-conserving CKM-suppressed mode ($\Delta C = -1,\ \Delta S = 0$) are of $\mathcal{O}(10^{-4}) \sim \mathcal{O}(10^{-5})$ for $B_c^+ \to \pi^+ B_1^{0(\prime)}$, and $B_c^+ \to \pi^0 B_1^+$ decays, respectively. While the decays involving $\eta^{(\prime)}$ states, *i.e.*, $B_c^+ \to \eta^{(\prime)} B_1^{+'}$ modes, are highly suppressed. Decays $B_c^+ \to \pi^+ B_1^{0'}/\pi^+ B_1^0$ come from the color-favored diagrams.

iii. It is interesting to note that the branching ratios of CKM-doubly-suppressed ($\Delta C = -1,\ \Delta S = 1$) Class I decays $B_c^+ \to K^+ B_1^{0(\prime)}$ and $B_c^+ \to K^0 B_1^{+'}$ are of $\mathcal{O}(10^{-6}) \sim \mathcal{O}(10^{-7})$.

iv. We wish to point out that for many of the decays, with branching ratios $\mathcal{O}(10^{-6})$ or less, the uncertainties appear to be large and are also sensitive to the choice of phenomenological parameters, like QCD coefficients, mixing angles, *etc*. We also noted that the uncertainties as large as 80% (seen in many decays) can reduce to less than 50% once we ignore the uncertainties in such parameters. Moreover, color-suppressed decay modes, being smaller in magnitude, are very sensitive to variation of the phenomenological parameters that lead to larger uncertainties. Therefore, we believe that such predictions of the branching ratios shall be seen as probable range.

It can be seen that many of the bottom-conserving decay modes have branching ratios comparable to $B_c \to PP/PV/VV$ decays that are well within the reach of current experiments. Since a large number of B_c events are expected from the LHCb; thus, $B_c \to B_s^{**} P$ decays will have a great potential to be observed. Observation of the bottom-conserving decays provides an ideal test

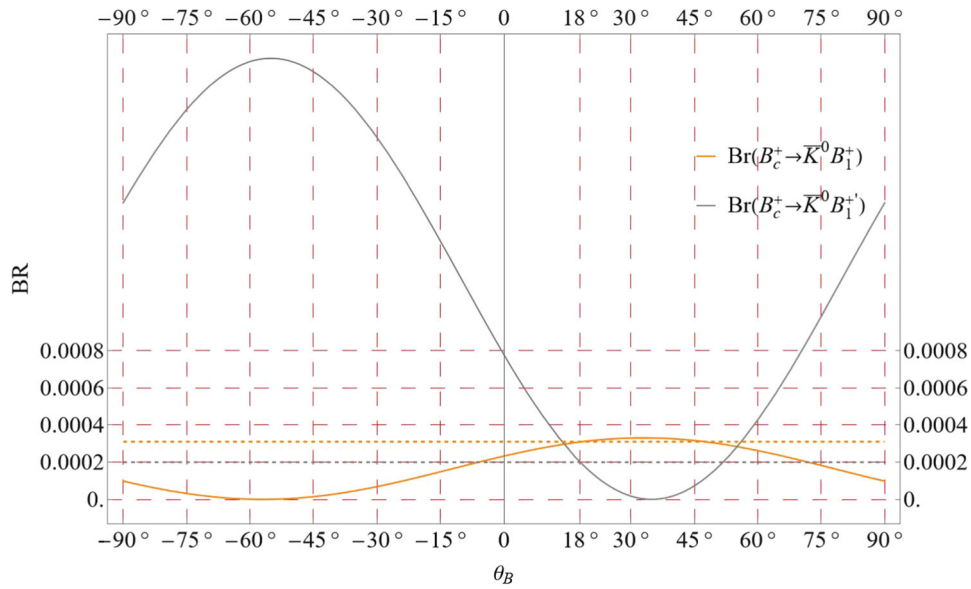

Fig. 2 Dependence of the branching ratios on mixing angle θ_B. Theoretical branching ratios are shown as dashed lines: orange and gray for $B_c^+ \to \bar{K}^0 B_1^+$ and $B_c^+ \to \bar{K}^0 B_1^{+'}$, respectively

for heavy quark theory and will further elucidate outstanding problems of the heavy quark states. Moreover, the study of excited heavy quark states has already attracted extensive experimental effort in order to understand their spectroscopy and decays.

4.2 Bottom-changing decay modes

In bottom-changing decays, we have analyzed B_s and B_c decays in ISGW II model using the HQS constraints. Aforementioned, in the nonrelativistic limit, ISGW II model provides an excellent opportunity to study $B_c(B_s) \to D_{(s)}$ transitions, where correspondingly large momentum transfer to the spectator $c-$quark takes place. It is worth mentioning that ISGW II model incorporates the $1/m_Q$ effects of HQS and HQET, resulting in more realistic form factors. Using the calculated form factors (as given in Tables 2 and 3), we obtain the branching ratios of $B_c(B_s)$ decays. We list our observations as follows:

4.2.1 CKM-favored, $\Delta C = 1$, $\Delta S = 0$ and $\Delta C = 0$, $\Delta S = -1$, modes

i. The most dominant decays, $\bar{B_s}^0 \to \pi^- D_{s1}^{+'}$, $\bar{B_s}^0 \to K^0 D_1^0$, and $\bar{B_s}^0 \to \pi^- D_{s1}^+$ have branching ratios $(7.2 \pm 2.7) \times 10^{-3}$, $(2.3 \pm 1.2) \times 10^{-3}$, and $(1.4 \pm 0.6) \times 10^{-3}$, respectively. The $\bar{B_s}^0 \to \pi^- D_{s1}^{+'}$ decay is color-favored, while $\bar{B_s}^0 \to K^0 D_1^0$ decay is color-suppressed. As mentioned earlier, the advantage of the nonleptonic B_s decays is that they are free from neutrino identification problem, and the products are identified in terms of well-known masses. The $B_s^0 \to D_s^{**}\pi$ decays are of great interest for being described by the pion-emission diagram only [12,32,73,79]. Moreover, the study of these decays would provide us an opportunity to understand the problem of smaller values of $j = 1/2$ form factors. Furthermore, these investigations can allow us to confirm the observations made in the respective nonstrange modes. The order of branching ratios for the CKM-favored B_s decays is $\mathcal{O}(10^{-3}) \sim \mathcal{O}(10^{-4})$. On the other hand, dominant B_c decays, $B_c^- \to D^0 D_1^{-'}/D^- D_1^0/D^- D_1^{0'}$, have branching ratios of $\mathcal{O}(10^{-4}) \sim \mathcal{O}(10^{-6})$. Here again, the uncertainties for some of the decays are as large as 60%, which can attributed mainly to uncertainties in form factors, mixing angles and QCD coefficients. It is well known that the broad resonances arising in D^{**} are always difficult to analyze, since the broadness of $D^{**}(j = 1/2)$ states is considered to be the source of these difficulties. However, the narrow $D^{**}(j = 3/2)$ states do not pose any serious problems [32,73,79,88]. Thus, the analyses of $B_c^- \to D^0 D_1^{-'}/D^- D_1^0/D^- D_1^{0'}$ could help to overcome such difficulties.

ii. In $(\Delta C = 0, \Delta S = -1)$ mode, dominant B_s decays involving $D_{s1}^{(\prime)}$ states, *i.e.*, $\bar{B_s}^0 \to D_s^+ D_{s1}^{-(\prime)}$ and $\bar{B_s}^0 \to D_s^- D_{s1}^{+(\prime)}$ have branching ratios $\mathcal{O}(10^{-2}) \sim \mathcal{O}(10^{-4})$. The decays involving D_s states (as the final product) are of immense importance for the verification of their properties via the analysis of their weak decays [89–91]. Thus, the production of these states from B_c and B_s weak decays could be ideal way to study their properties.

iii. For B_c meson, the $B_c^- \to \eta_c D_{s1}^{-(\prime)}$ decays having branching ratios $\mathcal{O}(10^{-3}) \sim \mathcal{O}(10^{-4})$ present an interesting opportunity to study Class III-type decays. These decays receive contribution from both the color-favored and color-suppressed diagrams, which interfere destructively to give smaller branching ratios. Further, it is worth remarking here that in heavy quark limit [3,5,88], the contributions from color-suppressed amplitudes are further suppressed by a factor of $1/m_Q$. However, the experiment in case of $B \to D\pi$ decays favors large contribution from the color-suppressed amplitude, which indicate the importance of nonfactorizable contributions [4]. Therefore, to highlight the significance of interference between color-favored and color-suppressed diagrams,

Table 11 Branching ratios for $B_c \to PA$ decays at large $N_c = 3$, $a_1 = 1.03 \pm 0.20$, and $a_2 = 0.11 \pm 0.10$

Decays	Branching ratios
$B_c^- \to \eta_c D_{s1}^-$	$(1.1 \pm 0.6) \times 10^{-3}$
$B_c^- \to \eta_c D_{s1}^{-\prime}$	$(3.6 \pm 2.4) \times 10^{-4}$
$B_c^- \to \eta_c D_1^-$	$(7.7 \pm 3.9) \times 10^{-5}$
$B_c^- \to \eta_c D_1^{-\prime}$	$(1.5 \pm 0.7) \times 10^{-5}$
$B_c^- \to D^- \bar{D}_1^0$	$(7.0 \pm 3.0) \times 10^{-8}$
$B_c^- \to D^- \bar{D}_1^{0\prime}$	$(2.8 \pm 1.1) \times 10^{-6}$
$B_c^- \to \bar{D}^0 D_1^-$	$(6.5 \pm 4.8) \times 10^{-7}$
$B_c^- \to \bar{D}^0 D_1^{-\prime}$	$(1.1 \pm 0.5) \times 10^{-7}$
$B_c^- \to D_s^- \bar{D}_1^0$	$(1.2 \pm 1.0) \times 10^{-7}$
$B_c^- \to D_s^- \bar{D}_1^{0\prime}$	$(7.3 \pm 2.8) \times 10^{-5}$
$B_c^- \to \bar{D}^0 D_{s1}^-$	$(9.3 \pm 2.7) \times 10^{-6}$
$B_c^- \to \bar{D}^0 D_{s1}^{-\prime}$	$(3.0 \pm 1.3) \times 10^{-6}$

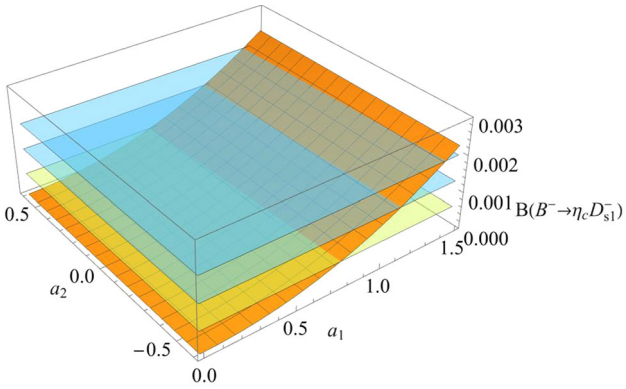

Fig. 3 Variation of the branching ratio of $B_c^- \to \eta_c D_{s1}^-$ with respect to a_1 and a_2 at mixing angle $\theta_{D_{s1}} = -5.7°$. The intersecting parallel planes correspond to the theoretical branching ratios with uncertainties

we have also calculated the branching ratios of Class III-type decays for $N_c = 3$, as shown in Table 11. In this case, the sign of a_2 has become positive, which results in constructive interference between color-favored and color-suppressed decay amplitudes; thus, branching ratios of decays involving A/A' are expected to enhance (decrease) corresponding to the sign of mixing angles.

iv In order to highlight the importance of color-favored and color-suppressed amplitudes and their mutual interference, we plot branching ratios of these decays with respect to a_1 and a_2 at mixing angle $\theta_{D_{s1}} = -5.7°$ as shown in Figs. 3 and 4. The intersecting parallel planes mark the upper and lower bounds of theoretical branching ratio about the central value. Figure 3 shows the dominance of color-favored amplitude corresponding to a_1 for $B_c^- \to \eta_c D_{s1}^-$ decay and is roughly independent of color-suppressed amplitude. This can also be confirmed from the value of branching ratio for the constructive interference, which is reduced owing to smaller a_1 for $N_c = 3$. However, Fig. 4 presents a very interesting scenario, where the branching ratio of $B_c^- \to \eta_c D_{s1}^{-\prime}$ decay not only favors smaller magnitude of a_2 but also negative sign for $a_1 \sim 1$. One can also notice large variation in the branching ratio corresponding to a_2, which indicate that $B_c^- \to \eta_c D_{s1}^{-\prime}$ is sensitive to the choice of QCD coefficients for a fixed mixing angle.

Furthermore, the phenomenological analyses of $B \to D^{**}\pi$ [70,74,88,92] indicate the requirement of, relatively, smaller magnitude of a_1, larger magnitude of a_2 terms with negative sign for a_1/a_2 to explain the existing experimental data [70,74]. Therefore, analyses and observation of $B_c \to D_{(s)}^{**} P$ decays can improve our current understanding of such outstanding puzzles. The rest of B_c decays in this mode are suppressed with branching ratios of $\mathcal{O}(10^{-8}) \sim \mathcal{O}(10^{-10})$.

4.2.2 CKM-suppressed, $\Delta C = 1, \Delta S = -1$ and $\Delta C = 0, \Delta S = 0$, modes

i. The dominant decays, $\bar{B_s}^0 \to K^- D_{s1}^{+(\prime)}$, $\bar{B_s}^0 \to D_s^+ D_1^-$ and $\bar{B_s}^0 \to D^- D_{s1}^{+\prime}$ have branching ratios $\mathcal{O}(10^{-4})$. The order of branching ratios for the rest of decays in the present mode is, $\mathcal{O}(10^{-5}) \sim \mathcal{O}(10^{-9})$. The decays, like $\bar{B_s}^0 \to \eta^{(\prime)} D_1^0$, $\bar{B_s}^0 \to D_s^+ D_1^{-\prime}$, $\bar{B_s}^0 \to D^- D_{s1}^+$, have branching ratios within the reach of current experiments.

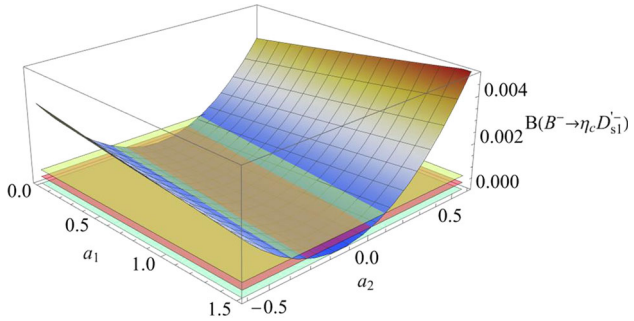

Fig. 4 Variation of the branching ratio of $B_c^- \to \eta_c D_{s1}^{-\prime}$ with respect to a_1 and a_2 at mixing angle $\theta_{D_{s1}} = -5.7°$. The intersecting parallel planes correspond to the theoretical branching ratios with uncertainties

ii. In the case of B_c decays, branching ratios of $B_c^- \to \eta_c D_1^{-(\prime)}$, $B_c^- \to D^0 D_{s1}^{-\prime}$, $B_c^- \to D_s^- D_1^0$, $B_c^- \to \pi^- \bar{D}_1^{0\prime}$, and $B_c^- \to \pi^0 D_1^{-\prime}$ are $\mathcal{O}(10^{-5}) \sim \mathcal{O}(10^{-6})$. The Class III $B_c^- \to \eta_c D_1^{-(\prime)}$ decays arise from the destructive interference of color-favored and color-suppressed diagrams. The branching $B_c^- \to \eta_c D_1^{-\prime}$ is enhanced while that of $B_c^- \to \eta_c D_1^-$ decay remains unchanged for the constructive interference at $N_c = 3$ case as shown in Table 11.

4.2.3 CKM-doubly-suppressed, $\Delta C = -1, \Delta S = -1$ and $\Delta C = -1, \Delta S = 0$, modes

i. Interestingly, the branching ratio of most dominant color-favored decay, $\bar{B}_s^{\,0} \to K^+ D_{s1}^-$ is $(2.5 \pm 1.5) \times 10^{-4}$. The next order decays $\bar{B}_s^{\,0} \to K^+ D_1^-$, $\bar{B}_s^{\,0} \to K^+ D_{s1}^{-\prime}$, $\bar{B}_s^{\,0} \to K^0 \bar{D}_1^0$, and $\bar{B}_s^{\,0} \to \eta^{(\prime)} \bar{D}_1^{0(\prime)}$, have branching ratios $\mathcal{O}(10^{-5}) \sim \mathcal{O}(10^{-6})$.
ii. It is worth noticing that all of the doubly-suppressed B_c decays in these modes belong to Class III. The color-favored and color-suppressed amplitudes interfere constructively to give the branching ratios $\mathcal{O}(10^{-5}) \sim \mathcal{O}(10^{-6})$ for some of the modes. Here again, the positive sign of the color-suppressed amplitude results in to constructive interference (see Table 11). Since the sign of color-suppressed diagrams is well-known puzzle in nonleptonic $B \to D_{(s)}^{**}\pi$ decays [12,89,92], observation of these modes can help to fix the sign and magnitude of the color-suppressed diagrams.

Although the axial-vector meson emitting decays have been studied in past, the heavy quark analysis has been ignored. Recently, the heavy quark symmetry and HQET effects have been studied on the form factors and semileptonic decays involving $B_s(B_c) \to D_{(s)}^{**}/B_s^{**}$ transitions [62–64,67]. However, less attention has been paid to study the nonleptonic decays to the best of our knowledge. Gang Li *et al.* [67] has studied the nonleptonic decays involving D_{s1} states in covariant light-front quark model in heavy quark limit. Their results for, $\bar{B}_s^{\,0} \to \pi^- D_{s1}^+ = 3.0 \times 10^{-5}$; $\bar{B}_s^{\,0} \to \pi^- D_{s1}^{+\prime} = 1.5 \times 10^{-3}$; $\bar{B}_s^{\,0} \to K^- D_{s1}^+ = 2.3 \times 10^{-6}$; $\bar{B}_s^{\,0} \to K^- D_{s1}^{+\prime} = 1.2 \times 10^{-4}$; $\bar{B}_s^{\,0} \to D^- D_{s1}^+ = 1.5 \times 10^{-6}$; $\bar{B}_s^{\,0} \to D^- D_{s1}^{+\prime} = 6.9 \times 10^{-5}$; $\bar{B}_s^{\,0} \to D_s^- D_{s1}^+ = 3.0 \times 10^{-5}$; $\bar{B}_s^{\,0} \to D_s^- D_{s1}^{+\prime} = 1.4 \times 10^{-3}$ compare well with our analysis.

5 Summary and conclusions

In this paper, we have studied the hadronic weak decays of bottom-charm and bottom-strange mesons emitting a pseudoscalar and an axial-vector mesons. We analyzed the charm and bottom axial-vector meson-emitting decays in ISGW II quark model and determined the $B_c(B_s) \to A/A'$ transition form factors in heavy quark symmetry constraints. These form factors are used to predict the branching ratios of nonleptonic weak $B_c(B_s) \to PA$ decays involving $c \to s/d$, $b \to c/s$ and $b \to u$ transitions in CKM-favored and CKM-suppressed modes. We draw the following observations:

1. The ISGW II model, in the light of heavy quark symmetry with the factorization hypothesis, can provide reliable predictions for the branching ratios of $B_c/B_s \to B_{s1}/D_{s1}P$ decays, specifically for the color-favored modes. The bottom-conserving $(B_c \to B_{(s)1})$ decays provide a peculiar case of heavy-to-heavy transitions where the whole momentum is carried by the heavy $b-$quark. The transition form factors in such case are best understood at maximum momentum transfer between the initial and final state, which are insensitive to $1/m_Q$ corrections in the zero recoil limit. Thus, we have predicted the branching ratios of the $B_c \to B_{(s)1}P$ decays at maximum momentum transfer in heavy quark limit. The predicted branching ratios of the dominant decays are as high as $\mathcal{O}(10^{-2}) \sim \mathcal{O}(10^{-4})$. Furthermore, these investigations could help us to understand the heavy quark dynamics of $B\pi$, BK, and $B_s\pi$ spectra, and the $B_s^{**}\pi$ states are of particular interest as they are expected to be a crucial product of the exotic hadrons [32–36]. It may be noted that the $B_{(s)1}^{**}$ widths are very sensitive to their masses, due to their proximity to the $B\pi/B^*\pi/BK/B^*K$ thresholds [37–39]. Precise measurement of these rates can resolve the fundamental problems concerning the nature of these states. Such decays are of immense importance to describe the heavy quark dynamics as well as physics beyond the standard model. Since the HQET helps to predict the properties of excited B and B_s mesons, thus, the observation of these heavy-to-heavy decay modes provides a vital test for the validity of heavy quark theory.

2. Proceeding in similar manner, we have calculated the branching ratio of the bottom-changing decays of B_c and B_s meson in heavy quark limit. Aforementioned, the ISGW II model incorporates the $1/m_Q$ effects of HQS and HQET giving more reliable predictions involving orbitally excited states. We have predicted the branching ratios for $B_c(B_s) \to P D_{(s)1}$ decays using the transition form factors at actual momentum transfer. The predicted branching ratios of several B_s decays lie in the range of $\mathcal{O}(10^{-2}) \sim \mathcal{O}(10^{-4})$. The branching predictions for dominant B_c decays are of $\mathcal{O}(10^{-3}) \sim \mathcal{O}(10^{-5})$.
3. Theoretically, $B_s \to D_s^{**}\pi$ decays are most interesting for being described by the pion emission diagram. Their branching ratios are also, $\mathcal{O}(10^{-3})$, large enough to be seen by current experiments. The analysis of such decays provides opportunities to probe the nature of $D_{s1}^{'}(2535)$ and $D_{s1}(2460)$ states and determines the axial-vector meson mixing using these nonleptonic decays. Similarly, the observation and analyses of $B_c \to D D_1$ type decays, whose branching ratios are $\mathcal{O}(10^{-4})$, can help resolving ambiguities surrounding $D^{**}(j = 1/2,\ 3/2)$ states.
4. We have calculated the branching ratios of Class III type B_c decays, both at large N_c limit and $N_c = 3$. The study of branching ratios of Class III type decays is important to fix the sign and magnitude of the color-suppressed amplitudes. It is well-known fact that the experimental data of $B \to D\pi$ decays favor a positive sign for a_2. More serious questions arise from the theoretical and phenomenological studies of $B \to D^{**}\pi$ decays in heavy quark limit which not only demands a negative sign but also the larger magnitude for a_2 to explain the existing experimental data. The study of Class III type B_c decays can not only help resolving such discrepancies but can also shed some light on the importance of nonfactorizable contributions in nonleptonic decays involving $p-$wave mesons.

We are expecting more experimental values from the LHCb and B factories *etc.* in the near future, which could help us to provide deeper insights into the $B_c(B_s)$ meson properties and their decays. Therefore, the experimental observation of such decays will help the heavy quark theory to assess underlying discrepancies of heavy flavor dynamics.

Acknowledgements One of the authors, RD, gratefully acknowledges the financial support by the Department of Science and Technology (SERB:CRG/2018/002796), New Delhi.

References

1. M. Wirbel, Prog. Part. Nucl. Phys. **21**, 33 (1988). https://doi.org/10.1016/0146-6410(88)90031-2
2. G. Buchalla, A.J. Buras, M.E. Lautenbacher, Rev. Mod. Phys. **68**, 1125 (1996). https://doi.org/10.1103/RevModPhys.68.1125. [arXiv:hep-ph/9512380]
3. M. Neubert, V. Riekert, Q.P. Xu, B. Stech, Exclusive weak decays of *B*-mesons, in *Heavy Flavors*, vol. 28, ed. by A.J. Buras, H. Linder (World Scientific, Singapore, 1992)
4. T.E. Browder, K. Honscheid, Prog. Part. Nucl. Phys. **35**, 81 (1995). https://doi.org/10.1016/0146-6410(95)00042-H. [arXiv:hep-ph/9503414]
5. M. Neubert, Phys. Rep. **245**, 259 (1994). https://doi.org/10.1016/0370-1573(94)90091-4. [arXiv:hep-ph/9306320]
6. M.J. Dugan, B. Grinstein, Phys. Lett. B **255**, 583 (1991). https://doi.org/10.1016/0370-2693(91)90271-Q
7. M.B. Wise, Nucl. Instrum. Meth. A **408**, 1 (1998). https://doi.org/10.1016/S0168-9002(98)00237-X. [arXiv:hep-ph/9803247]
8. N. Brambilla, S. Eidelman, C. Hanhart, A. Nefediev, C.P. Shen, C.E. Thomas, A. Vairo, C.Z. Yuan, arXiv:1907.07583 [hep-ex]; and references therein
9. N. Isgur, M.B. Wise, Phys. Rev. D **43**, 819 (1991). https://doi.org/10.1103/PhysRevD.43.819
10. I.I. Bigi, B. Blossier, A. Le Yaouanc, L. Oliver, O. Pene, J.-C. Raynal, A. Oyanguren, P. Roudeau, Eur. Phys. J. C **52**, 975 (2007). https://doi.org/10.1140/epjc/s10052-007-0425-1. [arXiv:0708.1621 [hep-ph]]
11. R.N. Faustov, V.O. Galkin, Phys. Rev. D **87**(3), 034033 (2013). https://doi.org/10.1103/PhysRevD.87.034033. [arXiv:1212.3167 [hep-ph]]
12. D. Becirevic, A. Le Yaouanc, L. Oliver, J.C. Raynal, P. Roudeau, J. Serrano, Phys. Rev. D **87**(5), 054007 (2013). https://doi.org/10.1103/PhysRevD.87.054007. [arXiv:1206.5869 [hep-ph]]
13. P. Colangelo, F. De Fazio, Phys. Rev. D **61**, 034012 (2000). https://doi.org/10.1103/PhysRevD.61.034012. [arXiv:hep-ph/9909423]
14. E.E. Jenkins, M.E. Luke, A.V. Manohar, M.J. Savage, Nucl. Phys. B **390**, 463 (1993). https://doi.org/10.1016/0550-3213(93)90464-Z. [arXiv:hep-ph/9204238]
15. G.R. Lu, Y.D. Yang, H.B. Li, Phys. Rev. D **51**, 2201 (1995). https://doi.org/10.1103/PhysRevD.51.2201
16. M.T. Choi, J.K. Kim, Phys. Lett. B **419**, 377 (1998). https://doi.org/10.1016/S0370-2693(97)01480-9. [arXiv:hep-ph/9805454]
17. R. Aaij et al. [LHCb Collaboration], Phys. Rev. Lett. **109**, 232001 (2012) https://doi.org/10.1103/PhysRevLett.109.232001 [arXiv:1209.5634 [hep-ex]]
18. R. Aaij et al. [LHCb Collaboration], Phys. Rev. Lett. **111**(18), 181801 (2013) https://doi.org/10.1103/PhysRevLett.111.181801[arXiv:1308.4544 [hep-ex]]
19. R. Aaij et al. [LHCb Collaboration], Phys. Rev. D **87**, 071103 (2013) https://doi.org/10.1103/PhysRevD.87.071103 [arXiv:1303.1737 [hep-ex]]
20. R. Aaij et al. [LHCb Collaboration], JHEP **1309**, 075 (2013) https://doi.org/10.1007/JHEP09(2013)075 [arXiv:1306.6723 [hep-ex]]
21. R. Aaij et al. [LHCb Collaboration], Phys. Rev. D **90**(3), 032009 (2014) https://doi.org/10.1103/PhysRevD.90.032009 [arXiv:1407.2126 [hep-ex]]
22. G. Aad et al. [ATLAS Collaboration], Phys. Rev. Lett. **113**(21), 212004 (2014) https://doi.org/10.1103/PhysRevLett.113.212004 [arXiv:1407.1032 [hep-ex]]
23. R. Aaij et al. [LHCb Collaboration], Phys. Rev. Lett. **114**, 132001 (2015) https://doi.org/10.1103/PhysRevLett.114.132001 [arXiv:1411.2943 [hep-ex]]
24. R. Aaij et al. [LHCb Collaboration], Phys. Rev. D **92**(7), 072007 (2015) https://doi.org/10.1103/PhysRevD.92.072007 [arXiv:1507.03516 [hep-ex]]
25. G. Aad et al. [ATLAS Collaboration], Eur. Phys. J. C **76**(1), 4 (2016) https://doi.org/10.1140/epjc/s10052-015-3743-8 [arXiv:1507.07099 [hep-ex]]
26. R. Aaij et al. [LHCb Collaboration], Phys. Rev. Lett. **118**(11), 111803 (2017) https://doi.org/10.1103/PhysRevLett.118.111803 [arXiv:1701.01856 [hep-ex]]
27. A.M. Sirunyan et al. [CMS Collaboration], Phys. Rev. Lett. **122**(13), 132001 (2019) https://doi.org/10.1103/PhysRevLett.122.132001 [arXiv:1902.00571 [hep-ex]]
28. R. Aaij et al. [LHCb Collaboration], Phys. Rev. Lett. **122**(23), 232001 (2019) https://doi.org/10.1103/PhysRevLett.122.232001 [arXiv:1904.00081 [hep-ex]]
29. A.V. Berezhnoy, I.N. Belov, A.K. Likhoded, A.V. Luchinsky, arXiv:1904.06732 [hep-ph]

30. T.A. Aaltonen et al. [CDF Collaboration], Phys. Rev. D **93**(5), 052001 (2016). https://doi.org/10.1103/PhysRevD.93.052001 [arXiv:1601.03819 [hep-ex]]
31. G. Chen, C.H. Chang, X.G. Wu, Phys. Rev. D **97**(11), 114022 (2018). https://doi.org/10.1103/PhysRevD.97.114022. [arXiv:1803.11447 [hep-ph]]
32. H.X. Chen, W. Chen, X. Liu, Y.R. Liu, S.L. Zhu, Rept. Prog. Phys. **80**(7), 076201 (2017). https://doi.org/10.1088/1361-6633/aa6420 [arXiv:1609.08928 [hep-ph]]; and references therein
33. V.M. Abazov et al. [D0 Collaboration], Phys. Rev. D **97**(9), 092004 (2018) https://doi.org/10.1103/PhysRevD.97.092004 [arXiv:1712.10176 [hep-ex]]
34. R. Aaij et al. [LHCb Collaboration], Phys. Rev. Lett. **117**(15), 152003 (2016). Addendum: [Phys. Rev. Lett. **118** (2017) no.10, 109904] https://doi.org/10.1103/PhysRevLett.118.109904, https://doi.org/10.1103/PhysRevLett.117.152003 [arXiv:1608.00435 [hep-ex]]
35. A.M. Sirunyan et al. [CMS Collaboration], Phys. Rev. Lett. **120**(20), 202005 (2018). https://doi.org/10.1103/PhysRevLett.120.202005 [arXiv:1712.06144 [hep-ex]]
36. W. Chen, H.X. Chen, X. Liu, T.G. Steele, S.L. Zhu, Phys. Rev. Lett. **117**(2), 022002 (2016). https://doi.org/10.1103/PhysRevLett.117.022002 [arXiv:1602.08916 [hep-ph]]
37. Z.G. Wang, Eur. Phys. J. C **76**(5), 279 (2016). https://doi.org/10.1140/epjc/s10052-016-4133-6. [arXiv:1603.02498 [hep-ph]]
38. V.M. Abazov et al. [D0 Collaboration], Phys. Rev. Lett. **117**(2), 022003 (2016). https://doi.org/10.1103/PhysRevLett.117.022003 [arXiv:1602.07588 [hep-ex]]
39. M. Aaboud et al. [ATLAS Collaboration], Phys. Rev. Lett. **120**(20), 202007 (2018). https://doi.org/10.1103/PhysRevLett.120.202007 [arXiv:1802.01840 [hep-ex]]
40. P.A. Zyla et al. [Particle Data Group], PTEP **2020**(8), 083C01 (2020) https://doi.org/10.1093/ptep/ptaa104
41. Y.-M. Wang, C.-D. Lu, Phys. Rev. D **77**, 054003 (2008). [arXiv:0707.4439 [hep-ph]]
42. X. Liu, Z.-J. Xiao, Phys. Rev. D **82**, 054029 (2010). [arXiv:1008.5201 [hep-ph]]
43. X. Liu, Z.-J. Xiao, Phys. Rev. D **81**, 074017 (2010). [arXiv:1001.2944 [hep-ph]]
44. X. Liu, Z.-J. Xiao, J. Phys. G **38**, 035009 (2011)
45. Z.-J. Xiao, X. Liu, Phys. Rev. D **84**, 074033 (2011). [arXiv:1111.6679 [hep-ph]]
46. N. Sharma, Phys. Rev. D **81**, 014027 (2010). [arXiv:1001.1851 [hep-ph]]
47. N. Sharma, R.C. Verma, Phys. Rev. D **82**, 094014 (2010). [arXiv:1004.1928 [hep-ph]]
48. N. Sharma, R. Dhir, R.C. Verma, J. Phys. G **37**, 075013 (2010). [arXiv:0911.3977 [hep-ph]]
49. C.-H. Chang, Y.-Q. Chen, G.-L. Wang, H.-S. Zong, Phys. Rev. D **65**, 014017 (2002). [arXiv:hep-ph/0103036]
50. G. Lopez Castro, H.B. Mayorga, J.H. Munoz, J. Phys. G **28**, 2241 (2002). [arXiv:hep-ph/0205273]
51. I. Bediaga, J.H. Munoz, arXiv:1102.2190 [hep-ph]
52. D. Ebert, R.N. Faustov, V.O. Galkin, Phys. Rev. D **82**, 034019 (2010). [arXiv:1007.1369 [hep-ph]]
53. Z.-h Wang, G.-L. Wang, C.-H. Chang, J. Phys. G **39**, 015009 (2012). [arXiv:1107.0474 [hep-ph]]
54. Z.-T. Zou, X. Yu, C.-D. Lu, Phys. Rev. D **87**, 074027 (2013)
55. R. Dhir, C.S. Kim, Phys. Rev. D **87**, 034004 (2013). [arXiv:1210.7890 [hep-ph]]
56. R. Dhir, C.S. Kim, Phys. Rev. D **88**(3), 034024 (2013). https://doi.org/10.1103/PhysRevD.88.034024. [arXiv:1307.0216 [hep-ph]]
57. F. Najafi, H. Mehraban, PTEP **2015**(3), 033B09 (2015). https://doi.org/10.1093/ptep/ptv001. [arXiv:1412.7951 [hep-ph]]
58. Z.T. Zou, Y. Li, X. liu, Phys. Rev. D **95**(1), 016011 (2017). https://doi.org/10.1103/PhysRevD.95.016011. [arXiv:1609.06444 [hep-ph]]
59. Z.T. Zou, Y. Li, X. Liu, Phys. Rev. D **97**(5), 053005 (2018). https://doi.org/10.1103/PhysRevD.97.053005. [arXiv:1712.02239 [hep-ph]]
60. Z. Rui, Phys. Rev. D **97**(3), 033001 (2018). https://doi.org/10.1103/PhysRevD.97.033001. [arXiv:1712.08928 [hep-ph]]
61. Z.Q. Zhang, H. Guo, N. Wang, H.T. Jia, Phys. Rev. D **99**(7), 073002 (2019). https://doi.org/10.1103/PhysRevD.99.073002. [arXiv:1903.03990 [hep-ph]]
62. N. Ghahramany, R. Khosravi, K. Azizi, Phys. Rev. D **78**, 116009 (2008). https://doi.org/10.1103/PhysRevD.78.116009. [arXiv:0811.2674 [hep-ph]]
63. R. Khosravi, Eur. Phys. J. C **75**(4), 170 (2015). https://doi.org/10.1140/epjc/s10052-015-3382-0. [arXiv:1502.01936 [hep-ph]]
64. Y.J. Shi, W. Wang, Z.X. Zhao, Eur. Phys. J. C **76**(10), 555 (2016). https://doi.org/10.1140/epjc/s10052-016-4405-1. [arXiv:1607.00622 [hep-ph]]
65. Q. Li, T. Wang, Y. Jiang, H. Yuan, T. Zhou, G.L. Wang, Eur. Phys. J. C **77**(1), 12 (2017). https://doi.org/10.1140/epjc/s10052-016-4588-5. [arXiv:1607.07167 [hep-ph]]
66. K.C. Yang, Phys. Rev. D **78**, 034018 (2008). https://doi.org/10.1103/PhysRevD.78.034018. [arXiv:0807.1171 [hep-ph]]
67. G. Li, F. l Shao, W. Wang, Phys. Rev. D **82**, 094031 (2010). https://doi.org/10.1103/PhysRevD.82.094031. [arXiv:1008.3696 [hep-ph]]
68. X.W. Kang, T. Luo, Y. Zhang, L.Y. Dai, C. Wang, Eur. Phys. J. C **78**(11), 909 (2018). https://doi.org/10.1140/epjc/s10052-018-6385-9. [arXiv:1808.02432 [hep-ph]]
69. Z.R. Liang, X.Q. Yu, arXiv:1903.07188 [hep-ph]
70. H.Y. Cheng, Phys. Rev. D **68**, 094005 (2003). https://doi.org/10.1103/PhysRevD.68.094005. [arXiv:hep-ph/0307168]
71. N. Isgur, D. Scora, B. Grinstein, M.B. Wise, Phys. Rev. D **39**, 799 (1989). and references therein
72. D. Scora, N. Isgur, Phys. Rev. D **52**, 2783 (1995). and references therein
73. H. Xu, Q. Huang, H.W. Ke, X. Liu, Phys. Rev. D **90**(9), 094017 (2014). https://doi.org/10.1103/PhysRevD.90.094017. [arXiv:1406.5796 [hep-ph]]
74. H.Y. Cheng, C.K. Chua, Phys. Rev. D **74**, 034020 (2006). https://doi.org/10.1103/PhysRevD.74.034020. [arXiv:hep-ph/0605073]
75. H.Y. Cheng, Phys. Lett. B **707**, 116 (2012)
76. M.C. Du, Q. Zhao, Phys. Rev. D **104**(3), 036008 (2021). https://doi.org/10.1103/PhysRevD.104.036008. [arXiv:2103.16861 [hep-ph]]
77. K. Abe et al., (Belle Collaboration), Phys. Rev. D **69**, 112002 (2004)
78. P. Colangelo et al., Phys. Lett. B **634**, 235 (2006)
79. Z.H. Wang, Y. Zhang, Th. Wang, Y. Jiang, Q. Li, G.L. Wang, Chin. Phys. C **42**(12), 123101 (2018). https://doi.org/10.1088/1674-1137/42/12/123101. [arXiv:1803.06822 [hep-ph]]
80. Q. li, R.H. Ni, X.H. Zhong, Phys. Rev. D **103**, 116010 (2021). https://doi.org/10.1103/PhysRevD.103.116010. [arXiv:2102.03694 [hep-ph]]
81. H.Y. Cheng, C.W. Chiang, Phys. Rev. D **81**, 074021 (2010). https://doi.org/10.1103/PhysRevD.81.074021. [arXiv:1001.0987 [hep-ph]]
82. H.Y. Cheng, C.W. Chiang, A.L. Kuo, Phys. Rev. D **91**(1), 014011 (2015). https://doi.org/10.1103/PhysRevD.91.014011 [arXiv:1409.5026 [hep-ph]] and references therein
83. H.Y. Cheng, C.K. Chua, C.W. Hwang, Phys. Rev. D **69**, 074025 (2004). https://doi.org/10.1103/PhysRevD.69.074025. [arXiv:hep-ph/0310359]
84. T. Feldmann, Int. J. Mod. Phys. A **15**, 159–207 (2000). https://doi.org/10.1142/S0217751X00000082. [arXiv:hep-ph/9907491 [hep-ph]]
85. D. Hatton et al. [HPQCD], Phys. Rev. D **102**(5), 054511 (2020). https://doi.org/10.1103/PhysRevD.102.054511 [arXiv:2005.01845 [hep-lat]]
86. R.C. Verma, J. Phys. G **39**, 025005 (2012). https://doi.org/10.1088/0954-3899/39/2/025005. [arXiv:1103.2973 [hep-ph]]
87. G.L. Wang, Phys. Lett. B **650**, 15–21 (2007). https://doi.org/10.1016/j.physletb.2007.05.001. [arXiv:0705.2621 [hep-ph]]
88. F. Jugeau, A. Le Yaouanc, L. Oliver, J.-C. Raynal, Phys. Rev. D **72**, 094010 (2005). [arXiv:hep-ph/0504206]

89. A. Faessler, T. Gutsche, S. Kovalenko, V.E. Lyubovitskij, Phys. Rev. D **76**, 014003 (2007). https://doi.org/10.1103/PhysRevD.76.014003. [arXiv:0705.0892 [hep-ph]]
90. J. Segovia, C. Albertus, E. Hernandez, F. Fernandez, D.R. Entem, Phys. Rev. D **86**, 014010 (2012). https://doi.org/10.1103/PhysRevD.86.014010. [arXiv:1203.4362 [hep-ph]]
91. L.F. Gan, J.R. Zhang, M.Q. Huang, H.B. Zhuo, Y.Y. Ma, Q.J. Zhu, J.X. Liu, G.B. Zhang, Eur. Phys. J. C **75**(5), 232 (2015). https://doi.org/10.1140/epjc/s10052-015-3449-y. [arXiv:1412.7969 [hep-ph]]
92. M. Atoui, B. Blossier, V. Morénas, O. Pène, K. Petrov, Eur. Phys. J. C **75**, 376 (2015). [arXiv:1312.2914 [hep-lat]]